International Journal of Nanomedicine

Dovepress
open access to scientific and medical research

Open Access Full Text Article

ORIGINAL RESEARCH

pH-sensitive PEGylation of RIPL peptide-conjugated nanostructured lipid carriers: design and in vitro evaluation

This article was published in the following Dove Press journal:
International Journal of Nanomedicine

Chang Hyun Kim[1,*]
Cheol-Ki Sa[1,*]
Min Su Goh[1]
Eun Seok Lee[1]
Tae Hoon Kang[1]
Ho Yub Yoon[1]
Gantumur Battogtokh[2]
Young Tag Ko[2]
Young Wook Choi[1]

[1]College of Pharmacy, Chung-Ang University, Seoul, Republic of Korea; [2]College of Pharmacy, Gachon University, Incheon, Republic of Korea

*These authors contributed equally to this work

Background: RIPL peptide (IPLVVPLRRRRRRRRC)-conjugated nanostructured lipid carriers (RIPL-NLCs) can facilitate selective drug delivery to hepsin (Hpn)-expressing cancer cells, but they exhibit low stability in the blood. Generally, biocompatible and nontoxic poly(ethylene glycol) surface modification (PEGylation) can enhance NLC stability, although this may impair drug delivery and NLC clearance. To attain RIPL-NLC steric stabilization without impairing function, pH-sensitive cleavable PEG (cPEG) was grafted onto RIPL-NLCs (cPEG-RIPL-NLCs).

Methods: Various types of NLC formulations including RIPL-NLCs, PEG-RIPL-NLCs, and cPEG-RIPL-NLCs were prepared using the solvent emulsification–evaporation method and characterized for particle size, zeta potential (ZP), and cytotoxicity. The steric stabilization effect was evaluated by plasma protein adsorption and phagocytosis inhibition studies. pH-sensitive cleavage was investigated using the dialysis method under different pH conditions. Employing a fluorescent probe (1,1′-dioctadecyl-3,3,3′,3′-tetramethylindocarbocyanine perchlorate [DiI]), in vitro drug delivery capacity of the cPEG-RIPL-NLCs under different pH conditions was also performed on Hpn-expressing SKOV3 cells and 3D-tumor spheroids.

Results: All prepared NLCs showed homogenous dispersion (<220 nm in size) with a negative ZP (−18 to −22 mV), except for positively charged RIPL-NLCs (~10 mV), revealing no significant cytotoxicity in either SKOV3 or RAW 264.7 cell lines. cPEG-RIPL-NLC protein adsorption was 1.75-fold less than that of RIPL-NLCs, and PEGylation significantly reduced the macrophage uptake. PEG detachment from the cPEG-RIPL-NLCs was pH-sensitive and time dependent. At 2 hours incubation, cPEG-RIPL-NLCs and PEG-RIPL-NLCs exhibited comparable cellular uptake at pH 7.4, whereas cPEG-RIPL-NLC uptake was increased over 2-fold at pH 6.5. 3D-spheroid penetration also demonstrated pH-sensitivity: at pH 7.4, cPEG-RIPL-NLCs could not penetrate deep into the spheroid core region during 2 hours, whereas at pH 6.5, high fluorescence intensity in the core region was observed for both cPEG-RIPL-NLC- and RIPL-NLC-treated groups.

Conclusion: cPEG-RIPL-NLCs are good candidates for Hpn-selective drug targeting in conjunction with pH-responsive PEG cleavage.

Keywords: cleavable PEG, cancer targeting, tumor spheroid, steric stabilization, cellular uptake

Correspondence: Young Wook Choi
College of Pharmacy, Chung-Ang University, 221 Heuksuk-dong, Dongjak-gu, Seoul 156-756, Republic of Korea
Tel +82 2 820 5609
Fax +82 2 826 3781
Email ywchoi@cau.ac.kr

Introduction

Nanoparticulate carriers including solid lipid nanoparticles and nanostructured lipid carriers (NLCs) have been widely used to deliver drug molecules to the target site and achieve desired biological functions.[1] These lipid-based nanocarriers have several advantages such as high payload of hydrophobic drugs, enhanced chemical stability

submit your manuscript | www.dovepress.com
Dovepress
http://dx.doi.org/10.2147/IJN.S184355

of the incorporated drugs, and ease of surface modification for targeted delivery.[2,3] Previously, we have introduced RIPL peptide (IPLVVPLRRRRRRRRC)-conjugated NLCs (RIPL-NLCs) to facilitate selective drug delivery to hepsin (Hpn)-expressing cancer cells.[4] As a lipid-based nanocarrier system, RIPL-NLCs composed of solid lipid and liquid oil showed high docetaxel-loading capacity and improved physical stability. In addition, via the surface modification with RIPL peptide that can recognize Hpn-overexpressing cells, RIPL-NLCs exhibited excellent Hpn-selectivity and enhanced drug internalization capacity. However, the major drawbacks of RIPL-NLCs include low stability against in vivo blood circulation by the reticuloendothelial system.

Following the intravenous administration of nanocarriers, nonspecific plasma proteins can bind to the nanocarrier surface, with the protein-adsorbed nanocarriers thence being easily recognized by the mononuclear phagocyte system and removed from the blood circulation.[5] This rapid removal of nanocarriers from the blood circulation constitutes a major obstacle to the potential use of nanocarriers as drug delivery systems.[6] To avoid the opsonization process and to impart longevity of the nanocarriers in blood circulation, surface modification with biocompatible and nontoxic poly(ethylene glycol) (PEGylation) has been widely utilized, providing a steric barrier that hinders unwanted interactions.[7] However, despite these advantages, recent studies have highlighted the drawbacks of PEGylation (so-called "PEG dilemmas"), including the hindrance of interaction between nanocarriers and cells at the pathological site, poor endosomal escape of nanocarriers, and accelerated blood clearance phenomenon upon repeated injection of PEGylated nanocarriers.[8,9]

To alleviate the PEG dilemmas, the employment of stimuli-sensitive cleavable PEG (cPEG), in which the protective PEG can be removed from the surface of nanocarriers under specific conditions, has been proposed. Stimuli-responsive mechanisms that trigger the cleavage process under the microenvironmental condition of the tumor include the use of acidic pH,[10–12] specific enzymes,[13–15] or reductive potential.[16–18] Among the proposed stimuli, acidic pH-sensitivity has been widely used in consideration of the inherent acidic tumor microenvironment. Unlike the normal physiological pH of 7.4, tumor tissues exhibit an extracellular pH in the range of 6.0–7.2[19] owing to the increased glycolysis and proton pump activity of tumor cells, which leads to the increased production of lactic acid.[20] To utilize this tumor acidic environment, several pH-sensitive bonds such as hydrazone (Hz), cis-acotinyl, acetal, and orthoester have been proposed.[21]

In this study, to attain steric stabilization of RIPL-NLCs in conjunction with the capacity of pH-responsiveness, a cPEG composed of a hydrophobic anchor bound to the PEG chain through a Hz bond was constructed and introduced for further surface modification. Various types of NLC formulations including RIPL-NLCs and PEGylated RIPL-NLCs were prepared and their physicochemical properties were characterized in terms of particle size, zeta potential (ZP), and microscopic morphology. The capacity for pH-sensitive cleavage was investigated under different pH conditions. Cytotoxicity of the various NLCs was estimated using macrophage (RAW 264.7) and tumor (SKOV3) cell lines. The steric stabilization effect was evaluated using protein adsorption and phagocytosis inhibition studies. The drug delivery capacity of the nanocarrier system under different pH conditions was also assessed in Hpn-expressing SKOV3 cell and tumor spheroid in vitro culture.

Materials and methods

Materials

Oleoyl macrogol-6 glycerides (Labrafil® M 1944 CS) and glyceryldistearate (Precirol® ATO 5) were acquired as a gift from Gattefosse (Saint-Priest, France). Dichloromethane (DCM), polysorbate 20 (Tween® 20), polyvinylalcohol, 1,1′-dioctadecyl-3,3,3′,3′-tetramethylindocarbocyanine perchlorate (DiI), PBS tablets, micro BCA protein assay kit, and N-(ε-maleimidocaproic acid) hydrazide (trifluoroacetic acid salt) (EMCH) were purchased from Sigma-Aldrich Chemical Co. (St Louis, MO, USA). 1,2-Distearoyl-sn-glycero-3-phosphoethanolamine-*N*-[maleimide(polyethylene glycol)-2000] (ammonium salt) (DSPE-PEG_{2000}-Mal), 1,2-distearoyl-sn-glycero-3-phosphoethanolamine-N-[methoxy(polyethylene glycol)-3000] (DSPE-PEG_{3000}), and 1,2-dipalmitoyl-sn-glycero-3-phosphothioethanol (sodium salt) (DPPE-SH) were purchased from Avanti Polar Lipids (Alabaster, AL, USA). $mPEG_{3000}$-butyraldehyde ($mPEG_{3000}$-CHO) was purchased from JenKem Technology (Beijing, People's Republic of China). The RIPL peptide was synthesized by Peptron Co. (Daejeon, Korea). For cell experiments, cell lines were purchased from the Korean Cell Line Bank (Seoul, Korea). PBS solution (pH 7.4, 10×) and cell culture materials including RPMI-1640 medium, DMEM, FBS, penicillin–streptomycin, and trypsin-EDTA (0.25%) were obtained from Invitrogen (Carlsbad, CA, USA). All other chemicals and reagents purchased from commercial sources were of analytical or cell culture grade.

Synthesis of DSPE-PEG$_{2000}$-RIPL

DSPE-PEG$_{2000}$-RIPL was prepared using the thiol-maleimide reaction by conjugating the cysteine residue of the RIPL peptide to DSPE-PEG$_{2000}$-Mal according to previous reports, with slight modification.[22,23] Briefly, 8.5 µmol of DSPE-PEG$_{2000}$-Mal and 9.5 µmol of RIPL peptide were dissolved in 2 mL of 0.01 M PBS (pH 7.4). The mixture was stirred gently at 25°C for 48 hours, then placed in a dialysis bag (3.5 kDa MWCO, Biotech CE Tubing; Spectrum Laboratories, Inc., Rancho Dominguez, CA, USA) and dialyzed against deionized water for 24 hours to remove the unconjugated peptides. The final solution in the dialysis bag was lyophilized and stored at −20°C until use. The final resulting DSPE-PEG$_{2000}$-RIPL was confirmed by matrix-assisted laser desorption ionization mass spectrometry time-of-flight mass spectrometer (MALDI-TOF MS) (Voyager-DE™ STR Biospectrometry Workstation; Applied Biosystems Inc., Langen, Germany). The DSPE-PEG$_{2000}$-RIPL yielded a unimodal peak at high molecular position (observed molecular weight [MW]=5,032.40 Da, calculated MW=5,042.62 Da).

Synthesis of DPPE-Hz-PEG$_{3000}$

As depicted in Figure 1A, DPPE-Hz-PEG$_{3000}$ as a cPEG was synthesized based on a previously published procedure with slight modification.[24] Briefly, DPPE-SH (35 mg, 49.1 µmol) was mixed with 25 mg (73.7 µmol) of EMCH in 3 mL anhydrous methanol containing 5 molar excess of triethylamine over lipid. The reaction was performed at 25°C under argon for 8 hours and monitored by thin-layer chromatography. Following solvent removal under reduced pressure, the residue was dissolved in DCM and applied to a 5-mL silica gel column that had been activated (150°C overnight) and prewashed with 20 mL of DCM. The column was equilibrated with an additional 15 mL of DCM followed by 5 mL of each of the following DCM/methanol mixtures: 4:0.25, 4:1, and 4:2, and, finally, with 6 mL of 4:3 v/v. The collected sample was dried under vacuum. Subsequently, 226.3 mg of mPEG$_{3000}$-CHO (73.65 µmol) in 2 mL of DCM was added to the obtained EMCH-activated phospholipid and stirred under argon overnight. The reaction mixture was dialyzed against water with pH 9–10 and distilled water for 48 hours, followed by freeze drying, which provided an 80% yield. Proton nucleic magnetic resonance (^{1}H NMR) spectra are shown in Figure 1B. ^{1}H NMR (600 MHz, $CDCl_3$) peaks were as follows: δ 0.86–0.89 (t, 6H, CH_3 of DPPE), 1.25 (m, 48H, DPPE), 1.58 (m, 8H, EMCH), 2.28–2.29 (m, 6H, EMCH and DPPE), 2.54 (m, 4, DPPE), 3.38 (m, 3H, CH_3O- of PEG), 3.52–3.56 (m, 8H, DPPE), 3.64 (m, 320H, PEG), 3.76 (m, 4H, DPPE), 3.96 (m, 5H, DPPE), 4.19 (m, 2H, DPPE), 4.4 (m, 1H, NH of PEG), and 5.3 (m, 1H, CH of DPPE).

Preparation of various NLC formulations

According to the previously published solvent emulsification–evaporation method,[4] four kinds of NLC formulations were prepared: plain NLCs (pNLCs), RIPL-NLCs, PEGylated RIPL-NLCs (PEG-RIPL-NLCs), and cleavable PEGylated RIPL-NLC (cPEG-RIPL-NLCs). For preparing pNLCs, Labrafil® M 1944 CS (liquid oil; 6.2 µL) and Precirol® ATO 5 (solid lipid; 15 mg) were dissolved in DCM (0.67 mL) as an organic phase, and then mixed with aqueous solution (4 mL) containing polysorbate20 (1%, w/v) and polyvinylalcohol (0.5%, w/v). Next, the mixture was homogenized at 15,000 rpm for 2 minutes using an Ultra-Turrax® T25 basic (IKA Labortechnik, Staufen, Germany) and the emulsion was sonicated using a probe-type sonicator (Sonoplus, HD 2070; Bandelin Electronics, Berlin, Germany) operating at 45% power for 3 minutes under cooling at 5°C. Finally, the emulsion was evaporated by magnetically stirring at 300 rpm for 1 hour with nitrogen gas purge to evaporate the organic phase. For preparing RIPL-NLCs, 1 mol% DSPE-PEG$_{2000}$-RIPL was dissolved in the aqueous phase, followed by the same procedure as above. Additionally, for the preparation of PEG-RIPL-NLCs and cPEG-RIPL-NLCs, 5 mol% DSPE-PEG$_{3000}$ and 5 mol% DPPE-Hz-PEG$_{3000}$ were dissolved in DCM, respectively, and mixed with the aqueous solution (pH adjusted with sodium phosphate dibasic), then processed using the same procedure as above. A representative schematic procedure for preparing cPEG-RIPL-NLCs is depicted in Figure 2A. Separately, to observe the cellular uptake of NLCs, DiI (a hydrophobic and red fluorescent probe) was loaded into NLCs (loading efficiency >98%; loading capacity 1.87±0.8 µg/mg) by dissolving in the organic phase. The unencapsulated DiI was purified by ultracentrifugation at 13,000× *g* for 20 minutes using Amicon® ultracentrifugal filters (MWCO 100 kDa; Millipore, Billerica, MA, USA). All prepared NLCs were stored at 4°C and used for subsequent experiments within 2 weeks.

Particle size and ZP measurements

Different NLCs were diluted 100-fold with distilled water and examined for the mean particle size, size distribution, and ZP using a dynamic light-scattering particle size analyzer (Zetasizer Nano-ZS; Malvern Instrument, Worcestershire, UK) equipped with a 50 mV laser at a scattering angle of 90°. Values were calculated from measurements performed in triplicate.

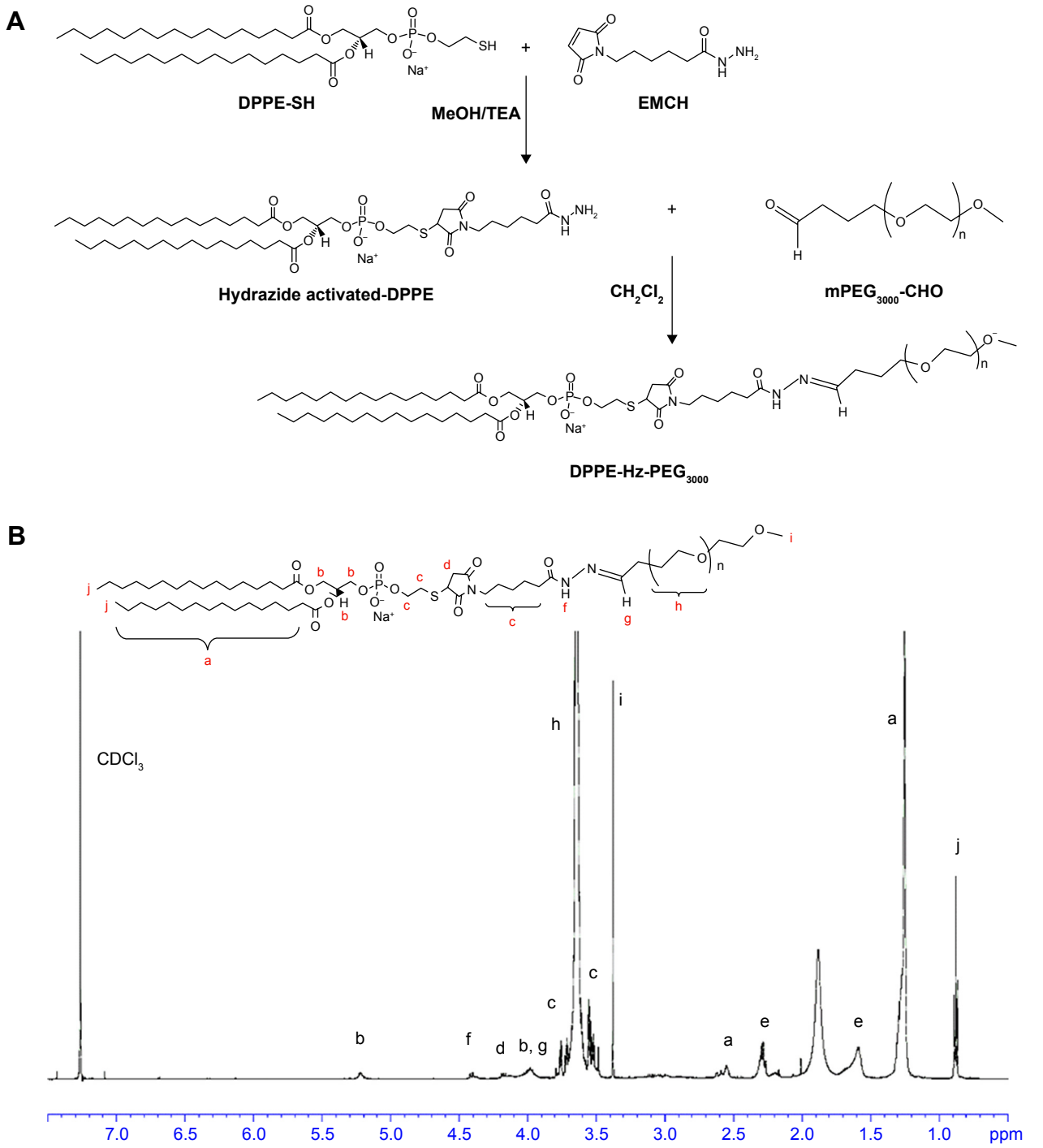

Figure 1 Synthesis of DPPE-Hz-PEG$_{3000}$.

Notes: (**A**) Scheme for synthesis of DPPE-Hz-PEG$_{3000}$ by a two-step reaction: (i) in anhydrous MeOH with TEA and (ii) in anhydrous dichloromethane. (**B**) Proton NMR spectrum of DPPE-Hz-PEG3000 conjugate in chloroform-d.

Abbreviations: DPPE-SH, 1,2-dipalmitoyl-sn-glycero-3-phosphothioethanol (sodium salt); MeOH, methanol; TEA, triethylamine; EMCH, N-(ε-maleimidocaproic acid) hydrazide (trifluoroacetic acid salt); mPEG-CHO, mPEG$_{3000}$-butyraldehyde; DPPE-Hz-PEG$_{3000}$, 1,2-dipalmitoyl-sn-glycero-3-phosphothioethanol-hydrazone-poly(ethylene glycol)$_{3000}$; NMR, nuclear magnetic resonance.

Transmission electron microscopy

The morphology of different NLCs was examined using a transmission electron microscope (JEM1010; JEOL, Tokyo, Japan) with an acceleration voltage of 80 kV. Prior to staining, samples were diluted 10-fold using distilled water and placed onto a carbon film covered with a copper grid. Further, according to the negative staining method,[25] the samples were stained with a drop of 2% phosphotungstic acid,

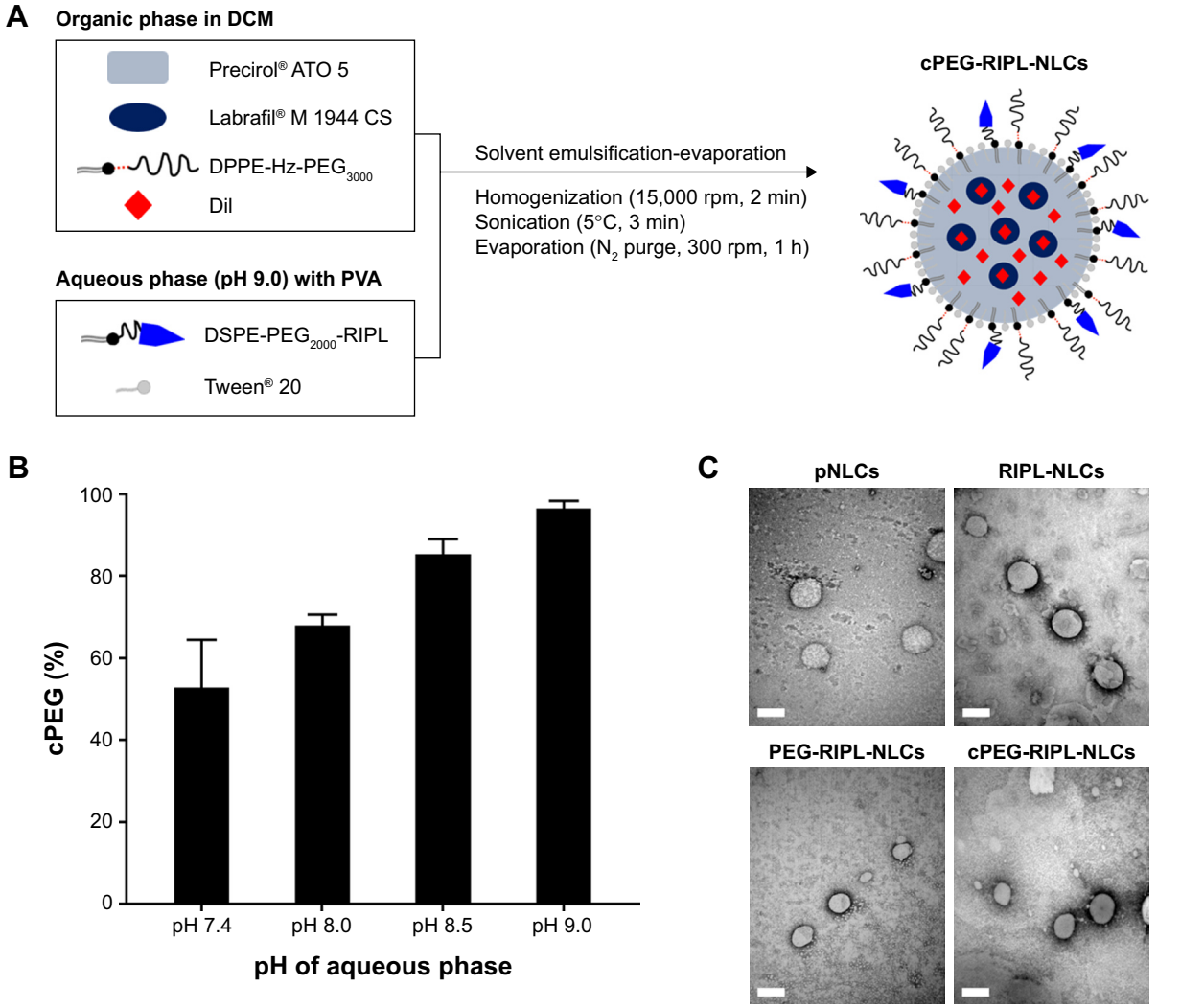

Figure 2 Preparation of cPEG-RIPL-NLCs and characterization of NLCs.
Notes: (**A**) Schematic procedures for preparing cPEG-RIPL-NLCs. (**B**) Degree of cPEGylation at different aqueous pH. Data represent the means±SD (n=3). (**C**) TEM images of pNLCs, RIPL-NLCs, PEG-RIPL-NLCs, and cPEG-RIPL-NLCs. Scale bars represent 200 nm.
Abbreviations: DCM, dichloromethane; DiI, 1,1′-dioctadecyl-3,3,3′,3′-tetramethylindocarbocyanine perchlorate; PVA, polyvinylalcohol; DPPE-Hz-PEG$_{3000}$, 1,2-dipalmitoyl-sn-glycero-3-phosphothioethanol-hydrazone-poly(ethylene glycol)$_{3000}$; DSPE-PEG$_{2000}$-RIPL, 1,2-distearoyl-sn-glycero-3-phosphoethanolamine-poly(ethylene glycol)$_{2000}$-RIPL peptide; NLCs, nanostructured lipid carriers; pNLCs, plain NLCs; RIPL-NLCs, RIPL peptide-conjugated NLCs; PEG-RIPL-NLCs, PEG-modified RIPL-NLCs; cPEG-RIPL-NLCs, cleavable PEG-modified RIPL-NLCs; TEM, transmission electron microscopy.

washed with distilled water, and dried at room temperature prior to observation.

pH-sensitive cleavage of cPEG-RIPL-NLCs

The acid sensitivity of the cPEG-RIPL-NLCs was evaluated using a dialysis method with slight modification.[11] Briefly, a dispersion of cPEG-RIPL-NLCs (750 µL) was randomly divided into dialysis bags (3.5 kDa MWCO). Subsequently, the dialysis bags were clipped with closures and completely soaked in PBS solution (30 mL) of different pH values (pH 5.0, 6.5, 7.4, and 8.5) at 37°C for 4 hours with gentle shaking at 100 rpm. At predetermined time points (15, 30, 60, 90, 120, and 480 minutes), an aliquot (1 mL) of sample solution was withdrawn and an equivalent volume of fresh PBS solution was replenished. The amount of the cleaved PEG in the sample solution was determined using a HPLC system (Waters® Corporation, Milford, MA, USA) consisting of separating modules (Waters® e2695), a refractive index detector (Waters® 2414), and a data station (Empower® 3). PEG was separated via a size exclusion column (PL aquagel-OH 20, 5 µm, 300×7.5 mm; Agilent Technologies, Inc., Santa Clara, CA, USA) with distilled water as a mobile phase delivering at a flow rate of 0.6 mL/min. The injection volume was 50 µL and the column temperature was maintained at 25°C.

Plasma protein adsorption assay

Physical stability and protein adsorption were investigated by measuring the amount of BSA bound to NLCs using a micro-BCA protein assay kit as previously reported.[26] Briefly, different NLC formulations were incubated with PBS solution (pH 7.4) containing BSA (250 μg/mL) at 37°C for predetermined time periods (0.5, 1, 2, and 4 hours) and the samples were centrifuged at 13,000× *g* for 30 minutes to remove the free BSA in the supernatant. Subsequently, the pellets were redispersed in 1 mL of PBS solution and vortexed at 2,000 rpm for 20 minutes. Following the redispersion, 150 μL of each sample was placed into 96-well plates, then mixed with 150 μL of BCA working reagent and incubated at 37°C for 30 minutes. The absorbance was measured spectrophotometrically at 562 nm using a microplate reader (FlexStation 3; Molecular Devices, Sunnyvale, CA, USA).

Cell culture

A human ovarian carcinoma cell line (SKOV3) and murine macrophage cell line (RAW 264.7) were cultured in RPMI-1640 medium and DMEM, respectively. Both media were supplemented with 10% FBS, 100 units/mL penicillin, and 100 μg/mL streptomycin. The cells were grown at 37°C in a humidified 5% CO_2 incubator. In all studies, the cells were subcultured every 2–3 days and were used for experiments at passages 5–20.

Cellular uptake study

Intracellular uptake behavior of NLCs to target cancer cells was investigated quantitatively by determining the mean fluorescence intensity (MFI) of DiI by flow cytometry using an FACSCalibur (Becton Dickinson, Bedford, MA, USA) equipped with a 488-argon-ion laser.[22] Briefly, SKOV3 cells (3×10^5 cells/well) were placed in 6-well plates with culture medium and incubated. After 24 hours, the medium was discarded, and the cells were washed twice with PBS solution. Subsequently, the cells were incubated with pH-adjusted (pH 7.4 or 6.5 using 0.1 N HCl) serum-free culture medium containing various NLCs at the final DiI concentration of 100 ng/mL. After incubation for 0.5 or 2 hours, the cells were washed twice with cold PBS solution, detached from the wells using trypsin-EDTA, and resuspended in 500 μL of PBS for analysis using a flow cytometer. A total of 10,000 cells were analyzed for each determination using the FL2 channel and the viable cells were gated for fluorescence analysis. Data were analyzed using BD Cell Quest Pro (Becton Dickinson). All experiments were performed in triplicate.

Confocal laser scanning microscopy (CLSM) observation

For qualitative analysis, SKOV3 cells were seeded onto a Lab-Tek II chamber slide with cover (Thermo Scientific Nunc, Rochester, NY, USA) at a density of 5×10^4 cells per well. After 24 hours, the medium was removed, and the cells were washed twice with PBS solution. Next, cells were incubated in culture medium at pH 7.4 or 6.5 containing different NLCs at DiI concentration of 100 ng/mL for 0.5 and 2 hours, and then washed twice with cold PBS solution and fixed with 4% paraformaldehyde for 20 minutes at 25°C. The cells were mounted by using Vectashield mounting medium containing DAPI (H-1200; Vector Laboratories, Inc., Burlingame, CA, USA). Finally, the cells were observed using a confocal microscope (Zeiss LSM 700 Meta; Carl Zeiss, Jena, Germany) under 400× magnification.

Macrophage phagocytosis study

In vitro macrophage phagocytosis behavior was also quantified using flow cytometry.[27,28] Briefly, RAW 264.7 cells were seeded in 6-well plates at a density of 2×10^5 cells/well with culture medium and allowed to adhere overnight. After 24 hours, the medium was discarded, and cells were washed twice with PBS solution. Further, the cells were incubated with serum-free culture medium (pH 7.4) containing DiI-loaded NLCs in which the concentration of DiI was 100 ng/mL. After 0.5 or 2 hours incubation, the cells were treated using the same procedure described in the cell uptake study.

Cytotoxicity assessment

The cytotoxicity of the different empty NLCs against SKOV3 and RAW 264.7 cells was determined by WST-1 assay.[29] Cells were cultured in 96-well plates at a density of 5×10^3 cells per well and allowed to adhere for 24 hours prior to the assay. Subsequently, the cells were incubated with culture medium containing different empty NLC concentrations (10, 50, and 100 ng/mL as DiI-equivalent) at 37°C for 24 and 48 hours. Culture medium was used as a blank control. Subsequently, the plates were incubated with 10% WST-1 reagents (EZ-cytox; Daeil Lab service, Seoul, Korea) for 30 minutes. The absorbance of WST formazan dye was assessed at 450 nm using a microplate reader. The experiments were conducted in triplicate and the relative viability of cells was determined as follows: relative cell viability (%)=$A_{treated}/A_{control}\times100$, where $A_{treated}$ and $A_{control}$ represent the absorbance of treated and control groups, respectively.

Tumor spheroid penetration study

Three-dimensional (3D) spheroids of tumor cells were established as previously described.[30] Briefly, SKOV3 cells were detached with trypsin-EDTA and passed through a 70-µm cell strainer to generate single-cell suspensions. To prepare 3D-spheroids, the SKOV3 single-cell suspension was transferred into a 96-well spheroid microplate (C.4515; Corning Inc., Kennebunk, ME, USA) at a density of 1×10^4 cells/200 µL per well. The plates were agitated gently for 5 minutes and cultured at 37°C. The formation of spheroids was monitored using an optical microscope at 40× magnification (KI-400; Optinity, Korea Labtech, Gyeonggi-do, Korea). After 4 days, when the size of spheroids reached 500 µm, the spheroids were incubated for 2 hours in culture medium at pH 7.4 or 6.5 containing different NLCs at a final DiI concentration of 100 ng/mL. Subsequently, 3D-spheroids were washed with PBS solution, fixed with 4% paraformaldehyde for 20 minutes, and placed into a Lab-Tek II chamber prior to imaging. Images were obtained using CLSM with a DiI filter (Ex/Em 549/565 nm) using the Z-stacking mode (z 1–8, slice thickness 15 µm) under 100× magnification.

Statistical analysis

All data are expressed as the means±SD. Differences between groups were analyzed by using a Student's *t*-test or ANOVA and considered to be significant at $P<0.05$.

Results and discussion

Physiochemical characteristics of NLCs

RIPL-NLCs were successfully prepared and characterized by measuring their particle size, polydispersity index (PDI), and ZP (Table 1). The mean particle size of all NLCs was below 220 nm as determined by dynamic light scattering. PDI was <0.3, indicating a narrow and homogenous size distribution. Although the particle size was slightly changed by encapsulation of DiI, the difference was not significant. The modification of RIPL and PEG onto the surface of NLCs resulted in a slight increase of particle size owing to the increased hydrodynamic diameter.[31] The ZP of all NLCs showed a negative charge in the range of −18 to −22 mV, except for RIPL-NLCs that showed a positive charge of ~+10 mV. The ZP was also slightly but not significantly changed by encapsulation of DiI. As we have previously reported, the positive charge of RIPL-NLCs could be attributed to the presence of the RIPL peptide, which contains positively charged octaarginine (R8);[22] the ZP reflects the exposed RIPL moieties on the carrier surface. In contrast, despite the presence of the RIPL peptide, PEGylated RIPL-NLCs were negatively charged, indicating that PEG coated the surface. This type of charge reversal or ZP reduction consequent to shielding by longer PEG chains has been frequently reported. For example, Koren et al described that a higher PEG shielding resulted in more negative ZP values for cell-penetrating TAT peptide-modified liposomes in a dose-dependent manner.[10] The ZP value of R8-modified liposomes was also strongly positive, whereas surface modification with PEG or thiolytic-cleavable PEG effected a change to a slightly negative charge.[32]

Because the cPEG moiety is pH-sensitively hydrolyzed, the pH of the aqueous phase should be carefully controlled during the cleavable PEGylation process. In the present study, to ensure the stability of cPEG during the preparation of cPEG-RIPL-NLCs, aqueous pH was adjusted to weak alkaline conditions of pH 7.4–9. As shown in Figure 2B, the degree of cPEGylation (the percentage of cPEG attached on the surface compared with the amount of cPEG added initially) increased as the aqueous pH increased: ~53% at pH 7.4, 68% at pH 8, 85% at pH 8.5, and >97% at pH 9. This result was in good consistency with an earlier report, in which PBS solution under pH 8.0 was used to hydrate pH-sensitive liposomes modified with PEG_{5000}-Hz-PE to reduce the hydrolysis during the preparation.[11] Therefore, the basic aqueous phase of pH 9.0 was subsequently used in the present study to prepare cPEG-RIPL-NLCs.

Table 1 Physicochemical characteristics of different NLCs

	Empty			DiI-loaded		
	Size (nm)	PDI	ZP (mV)	Size (nm)	PDI	ZP (mV)
pNLCs	195.2±1.5	0.187±0.018	−19.4±0.8	199.1±5.6	0.234±0.003	−18.4±1.0
RIPL-NLCs	215.1±4.5	0.259±0.026	9.5±1.8	216.2±6.6	0.241±0.010	10.4±1.1
PEG-RIPL-NLCs	208.2±2.9	0.294±0.025	−19.2±1.0	212.0±3.1	0.138±0.019	−20.1±0.9
cPEG-RIPL-NLCs	193.1±2.7	0.207±0.009	−19.3±1.0	192.4±4.2	0.226±0.002	−21.9±0.2

Note: Data represent the means±SD (n=3).

Abbreviations: DiI, 1,1′-dioctadecyl-3,3,3′,3′-tetramethylindocarbocyanine perchlorate; NLCs, nanostructured lipid carriers; PDI, polydispersity index; PEG-RIPL-NLCs, PEG-modified RIPL-NLCs; RIPL-NLCs, RIPL peptide-conjugated NLCs; ZP, zeta potential; cPEG-RIPL-NLCs, cleavable PEG-modified RIPL-NLCs; pNLCs, plain NLCs.

The transmission electron microscopy images of the various NLCs are shown in Figure 2C. All prepared NLCs were spherical in shape, representing a size of ~200 nm. Thus, we concluded that the surface modification with RIPL and PEG molecules did not change the morphological property of the NLCs.

pH-sensitive cleavage of cPEG-RIPL-NLCs

Hydrazone bonds are pH-labile linkers that may undergo protonation in a low-pH environment, leading to hydrolysis of the sensitive bond and therefore to detachment of the polymer molecule.[21] To verify such Hz bond cleavage of the cPEG-RIPL-NLCs, a pH-sensitivity assay was performed under four different pH conditions: pH 5.0, 6.5, 7.4, and 8.5. As shown in Figure 3, the detachment of PEG from the cPEG-RIPL-NLCs was time- and pH-dependent. After the incubation at pH 5.0 and 6.5, the hydrolysis percentage drastically increased over 80% and reached a plateau after 30 minutes incubation. In comparison, at pH 7.4, the hydrolysis rate was initially markedly reduced, resulting in <30% cleavage in 30 minutes, and then linearly increased up to 80% in 2 hours. At pH 8.5, the Hz bond was durable against the hydrolysis, showing an overall approximate cleavage of 30% after 4 hours.

Once nanocarriers including cPEG-RIPL-NLCs are passively accumulated in tumor sites via enhanced permeability and retention effects, pH-sensitive cleavage of PEG is expected to occur rapidly in the acidic extracellular tumor microenvironment. Previously, Ding et al modified a liposome with Stearate-Hz-mPEG2000 and analyzed the pH-sensitivity by separating liposomes and cleaved PEG using HPLC.[12] They observed strong pH-sensitivity at pH 6.5, resulting in complete PEG cleavage after 30 minutes incubation. In addition, in another study, ~70% of PEG5K-Hz-PE was hydrolyzed under pH 6.0 in 2 hours.[11] In the present study, cPEG-RIPL-NLCs also exhibited pH-sensitive hydrolysis at an acidic pH below 6.5. However, the detachment of PEG at physiological conditions (pH 7.4) was also observed. This unexpected cleavage of PEGs might be attributable to the unstable Hz bond, as reported elsewhere.[24,33] Specifically, when the pH-sensitive cleavage was measured based on the disappearance of the HPLC peak of micelles composed of cPEG conjugate, the half-life of the micelle at pH 7.4 was ~2 hours. cPEG conjugates derivatized from aliphatic aldehyde were more readily hydrolyzed than those from aromatic aldehyde owing to the poor attribution to π bonds of the −C=N of the Hz bond.[24] In the present experiment, as EMCH was used as an acyl hydrazide linker, which contains an aliphatic aldehyde, cPEG (DPPE-Hz-PEG$_{3000}$) might be relatively unstable at physiological pH. However, considering the high blood flow in the human body, it would be expected that a reasonable fraction of cPEG-RIPL-NLCs could reach the target tissue before the complete cleavage of PEG from the NLC formulations.

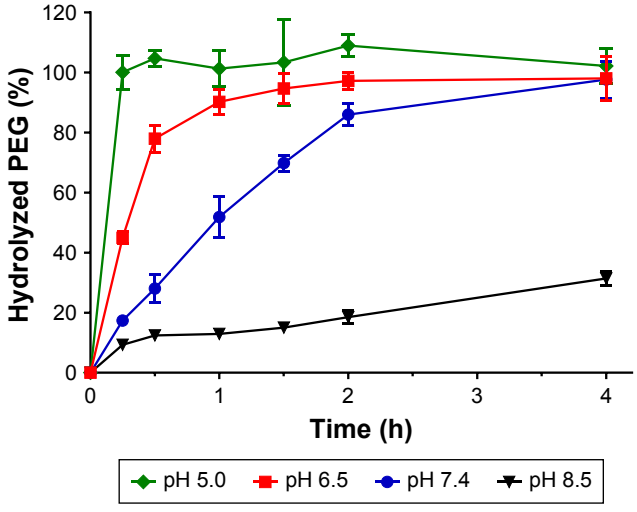

Figure 3 pH-sensitive cleavage of cPEG-RIPL-NLCs in different pH conditions (n=3).
Abbreviations: PEG, poly(ethylene glycol); cPEG-RIPL-NLCs, cleavable PEG-modified RIPL-NLCs.

Plasma protein adsorption assay

The anti-adsorption behavior of PEGylated RIPL-NLCs in BSA solution was measured using the BCA protein assay to estimate the in vivo stability of the nanocarriers. As BSA is the most abundant protein in serum, it was selected as a model plasma protein.[34] As shown in Figure 4, the amount of protein adsorbed onto pNLCs after 4 hours was 11.8±1.2 μg (~4% of initially added BSA), whereas that of RIPL-NLCs was 69.4±3.8 μg (~27%). This high protein adsorption property of RIPL-NLCs may be mainly due to the van der Waals interaction between the plasma protein and the positively charged RIPL peptide.[35] In contrast, PEGylated RIPL-NLCs showed a significant reduction of BSA adsorption: compared with RIPL-NLCs, PEG-RIPL-NLCs (P=0.0001) and cPEG-RIPL-NLCs (P=0.0001) showed ~1.97- and 1.75-fold less protein adsorption at 2 hours. In particular, the protein adsorption pattern of PEG-RIPL-NLCs and cPEG-RIPL-NLCs was similar for the first 2 hours, but became different by 4 hours, indicating that the adsorption of cPEG-RIPL-NLCs was greater than that of PEG-RIPL-NLCs with significant difference at P<0.001. This behavior might be closely related to the time-dependent PEG cleavage as described above: upon

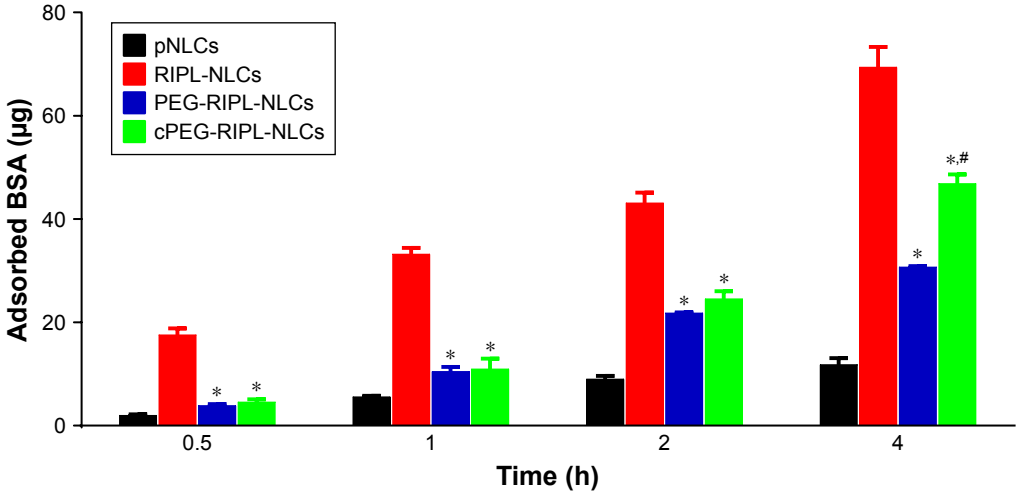

Figure 4 Serum protein adsorption onto the NLC samples in 250 µg/mL BSA solution.
Notes: Statistical analysis was performed using a Student's *t*-test (*$P<0.05$ vs RIPL-NLCs; #$P<0.05$ vs PEG-RIPL-NLCs).
Abbreviations: NLC, nanostructured lipid carrier; pNLCs, plain NLCs; RIPL-NLCs, RIPL peptide-conjugated NLCs; PEG-RIPL-NLCs, PEG-modified RIPL-NLCs; cPEG-RIPL-NLCs, cleavable PEG-modified RIPL-NLCs.

cleavage, the RIPL peptide could be exposed externally on the nanocarrier surface.

This stealth effect by PEG might be explained by several mechanisms, including that the steric repulsion and high mobility of longer PEG or cPEG chains may have prevented the RIPL peptide from interacting with serum proteins.[36] PEG chains of MW 1,500–5,000 Da with a grafting density of 5–10 mol% are generally accepted as showing an efficient stealth effect.[8,37] Based on the density of the PEG chains conjugated to the nanocarrier, PEG chains would acquire a different conformation; ie, a "mushroom" conformation if the grafting density is low (up to 4 mol%), whereas a "brush" conformation would be exhibited if the grafting density is higher.[10] The ideal coverage has been described as intermediate between these configurations.[36] Thus, considering the MW, coverage density, and the confirmation of PEG, the modification 5 mol% of PEG_{3000} was considered to achieve efficient surface coverage of RIPL-NLCs.

In vitro cell uptake study

A cellular uptake study was performed under different pH conditions to evaluate how the drug delivery capacity of cPEG-RIPL-NLCs changes upon pH-sensitive Hz bond cleavage. Based on the pH-sensitivity assay, test conditions were selected as follows: culture media of pH 6.5 and 7.4 to mimic the tumor microenvironment and normal physiological conditions, respectively, and incubation periods of 30 minutes and 2 hours to represent early and late time points. As shown in the flow cytometry histogram (Figure 5A), the degree of fluorescence peak shift was measured in the order of RIPL-NLCs>cPEG-RIPL-NLCs>PEG-RIPL-NLCs>pNLCs in all conditions. For quantitative comparison of the histogram shift, MFI was adopted as a parameter for graphical conversion. The cPEG-RIPL-NLCs showed a pH-dependence in cell uptake during both incubation periods, whereas other NLCs (pNLCs, RIPL-NLCs, and PEG-RIPL-NLCs) showed no pH-dependency. However, this difference was not time dependent. Over time, the level of MFI values increased, whereas the pattern for pH-sensitivity remained the same. In particular, RIPL-NLCs exhibited the greatest cellular uptake: over 3- or 2-times than that of pNLCs or PEG-RIPL-NLCs, respectively, regardless of the medium pH and incubation time. In addition, at pH 7.4, cell uptake of cPEG-RIPL-NLCs was similar to that of PEG-RIPL-NLCs. As expected, at pH 6.5, cell uptake of cPEG-RIPL-NLCs increased over 2-times compared with that of PEG-RIPL-NLCs, indicating the deshielding of PEG coat, allowing RIPL peptide extrusion on the nanocarrier surface. However, this recovery was incomplete because cell uptake of cPEG-RIPL-NLCs was less than that of intact RIPL-NLCs. This is probably due to residual PEG on the surface of the nanocarriers.[11]

Confocal microscopy observation provided further evidence for this effect (Figure 5B). Unlike pNLCs, all surface-modified NLCs (RIPL-NLCs, PEG-RIPL-NLCs, and cPEG-RIPL-NLCs) exhibited a time-dependent uptake pattern regardless of the medium pH. Notably, RIPL-NLCs were greatly internalized by SKOV3 cells owing to the cell-penetrating effect of RIPL peptide. Although the fluorescence intensity of PEG-RIPL-NLCs was weaker than that of RIPL-NLCs, it was still stronger than that of pNLCs. In comparison,

unlike the images of PEG-RIPL-NLCs, the fluorescence intensity of cPEG-RIPL-NLCs was time- and pH-dependent: at 0.5 hour, no differences were found in either pH; at 2 hours, the fluorescence was eminent in pH 6.5 medium, whereas only a slight increase was observed in pH 7.4 medium. The increased uptake of RIPL-NLCs likely occurred because of cell-penetrating and homing function of the RIPL peptide, as previously reported.[4] RIPL peptide-conjugation on the surface of NLCs enables the selective binding to Hpn owing to the IPL sequence and enhances the intracellular uptake via R8. The cellular uptake of RIPL-NLCs was dependent on Hpn expression. Stronger uptake in Hpn-positive cells than in Hpn-negative cells indicated that the surface modification with the RIPL peptide exhibited a better selective binding affinity of the nanocarrier to the extracellular membrane of Hpn-expressing cells.[4,29] Thus, we concluded that cPEG-RIPL-NLCs could promote the intracellular uptake based on the pH-sensitive cleavage of the PEG coating and de-shielding of the RIPL peptide on the NLC surface. Following PEG cleavage, cPEG-RIPL-NLCs are expected to show better selectivity to Hpn-expressing cells being internalized through endocytosis mediated by the R8 sequence of the RIPL peptide.[10,38]

Phagocytosis inhibition study

Using a murine macrophage cell line (RAW 264.7), phagocytosis inhibition of various NLCs was observed (Figure 6). Similar to the cell uptake study, DiI was employed

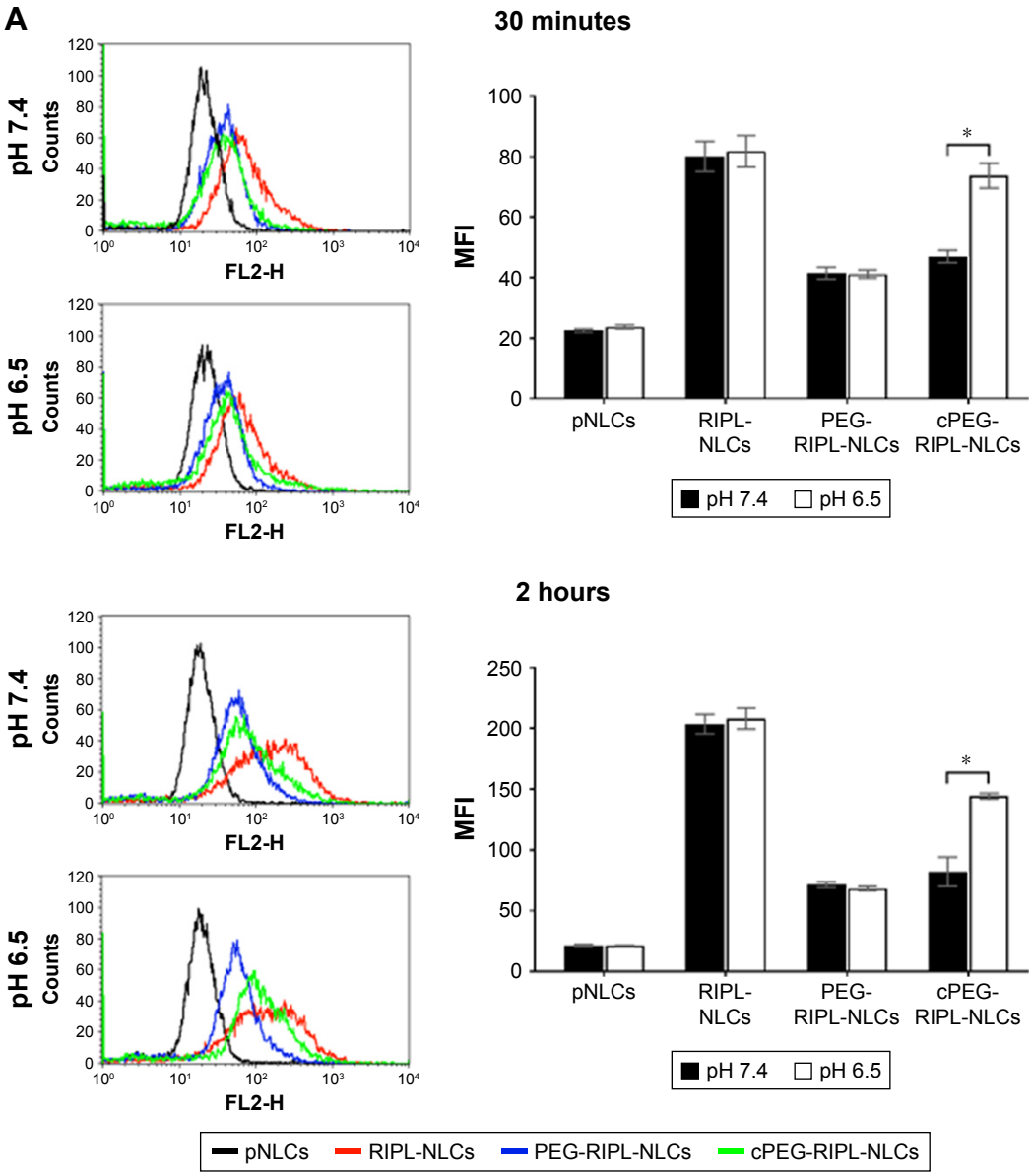

Figure 5 (*Continued*)

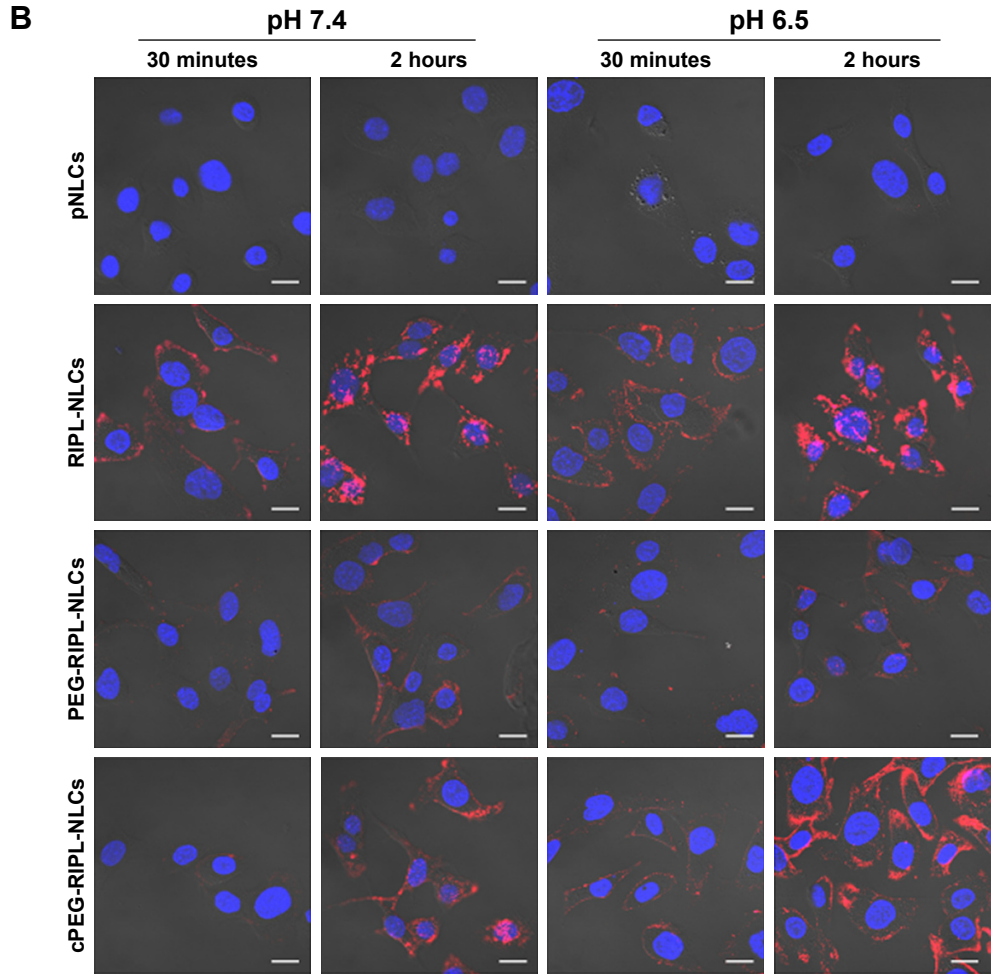

Figure 5 Quantitative and qualitative analysis of the cellular uptake of DiI-loaded NLC formulations under pH 6.5 and pH 7.4 for different time.
Notes: Concentration of DiI was 100 ng/mL. (**A**) Flow cytometry histogram showing the treatment effect: cells treated with pNLCs (black), RIPL-NLCs (red), PEG-RIPL-NLCs (blue), and cPEG-RIPL-NLCs (green). Data represent the means±SD (n=3). Statistical analysis was performed using a Student's *t*-test (*$P<0.05$ between different pH treatments). (**B**) Confocal microscopy images of SKOV3 cells incubated with pNLCs, RIPL-NLCs, PEG-RIPL-NLCs, and cPEG-RIPL-NLCs at 37°C for 30 minutes or 2 hours under pH 6.5 or 7.4. The nuclei were stained with DAPI for blue fluorescence and merged with bright field view and red fluorescence of DiI distributed in the cytoplasm. Scale bar represents 20 μm.
Abbreviations: MFI, mean fluorescence intensity; DiI, 1,1′-dioctadecyl-3,3,3′,3′-tetramethylindocarbocyanine perchlorate; NLC, nanostructured lipid carrier; pNLCs, plain NLCs; RIPL-NLCs, RIPL peptide-conjugated NLCs; PEG-RIPL-NLCs, PEG-modified RIPL-NLCs; cPEG-RIPL-NLCs, cleavable PEG-modified RIPL-NLCs.

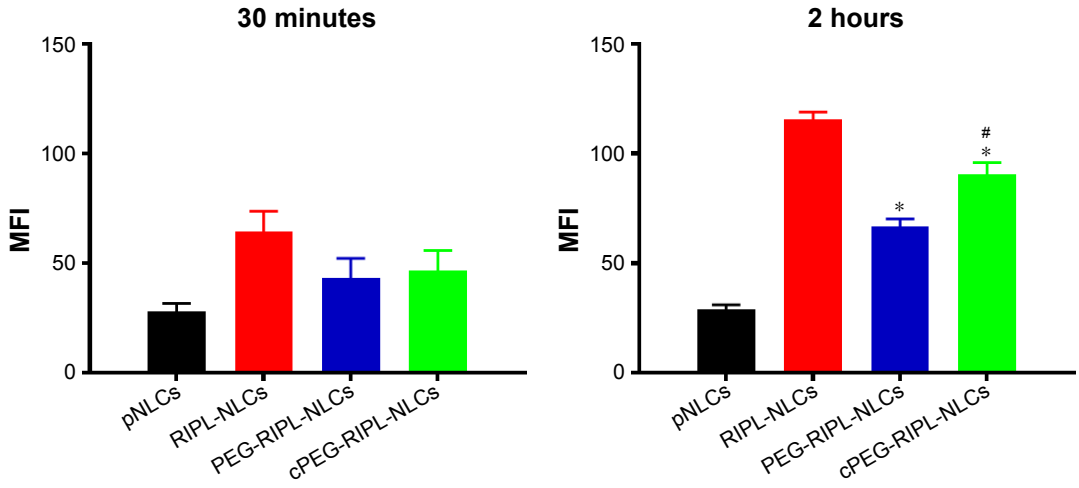

Figure 6 Flow cytometry analysis of phagocytosed NLC samples by RAW 264.7 cells after incubation for 30 minutes and 2 hours.
Notes: Statistical analysis was performed using a Student's *t*-test (*$P<0.05$ vs RIPL-NLCs; #$P<0.05$ vs PEG-RIPL-NLCs). Data represent the means±SD (n=3).
Abbreviations: MFI, mean fluorescence intensity; NLC, nanostructured lipid carrier; pNLCs, plain NLCs; RIPL-NLCs, RIPL peptide-conjugated NLCs; PEG-RIPL-NLCs, PEG-modified RIPL-NLCs; cPEG-RIPL-NLCs, cleavable PEG-modified RIPL-NLCs.

as a red fluorescent probe and MFI values were compared at 30 minutes and 2 hours. In the case of pNLCs (control), macrophage uptake was negligible and time dependent. This phagocytosis avoidance was attributable to their composition, including polysorbate 20, which stabilized the surface of pNLCs by mimicking the PEG action.[39] In contrast, surface-modified NLCs (RIPL-NLCs, PEG-RIPL-NLCs, and cPEG-RIPL-NLCs) revealed greater phagocytosis than pNLCs. Specifically, RIPL-NLCs were highly phagocytosed by macrophages, probably owing to the opsonizing tendency as described previously. However, as expected, macrophage uptake was markedly reduced by PEGylation of RIPL-NLCs. This suggested that both PEG and cPEG chains attract water molecules to create a hydrophilic barrier around the surface of RIPL-NLCs to inhibit phagocytosis by masking macrophage recognition.[40] Moreover, after 2 hours incubation, MFI values of cPEG-RIPL-NLCs were markedly increased, revealing a significant difference ($P<0.001$) vs those of PEG-RIPL-NLCs, possibly owing to a phenomenon whereby the PEG coating on cPEG-RIPL-NLCs was partially decomposed in the culture medium over time. This is consistent with the results of pH-sensitive cleavage, in which the Hz bond of cPEG was considerably hydrolyzed over time in pH 7.4 medium.

Cytotoxicity of various NLCs

The cytotoxicity of the empty NLCs was evaluated against SKOV3 and RAW 264.7 cell lines (Figure 7). The cell viability in the untreated control group was considered as 100%. Regardless of the cell type, all empty NLCs revealed no significant cell death in the concentration range used in this experiment. There were no significant differences in cytotoxicity between 24 h- and 48 h-incubation, even though a little deviation occurred in longer time incubation with SKOV3 cells. At DiI-equivalent concentration of 100 ng/mL

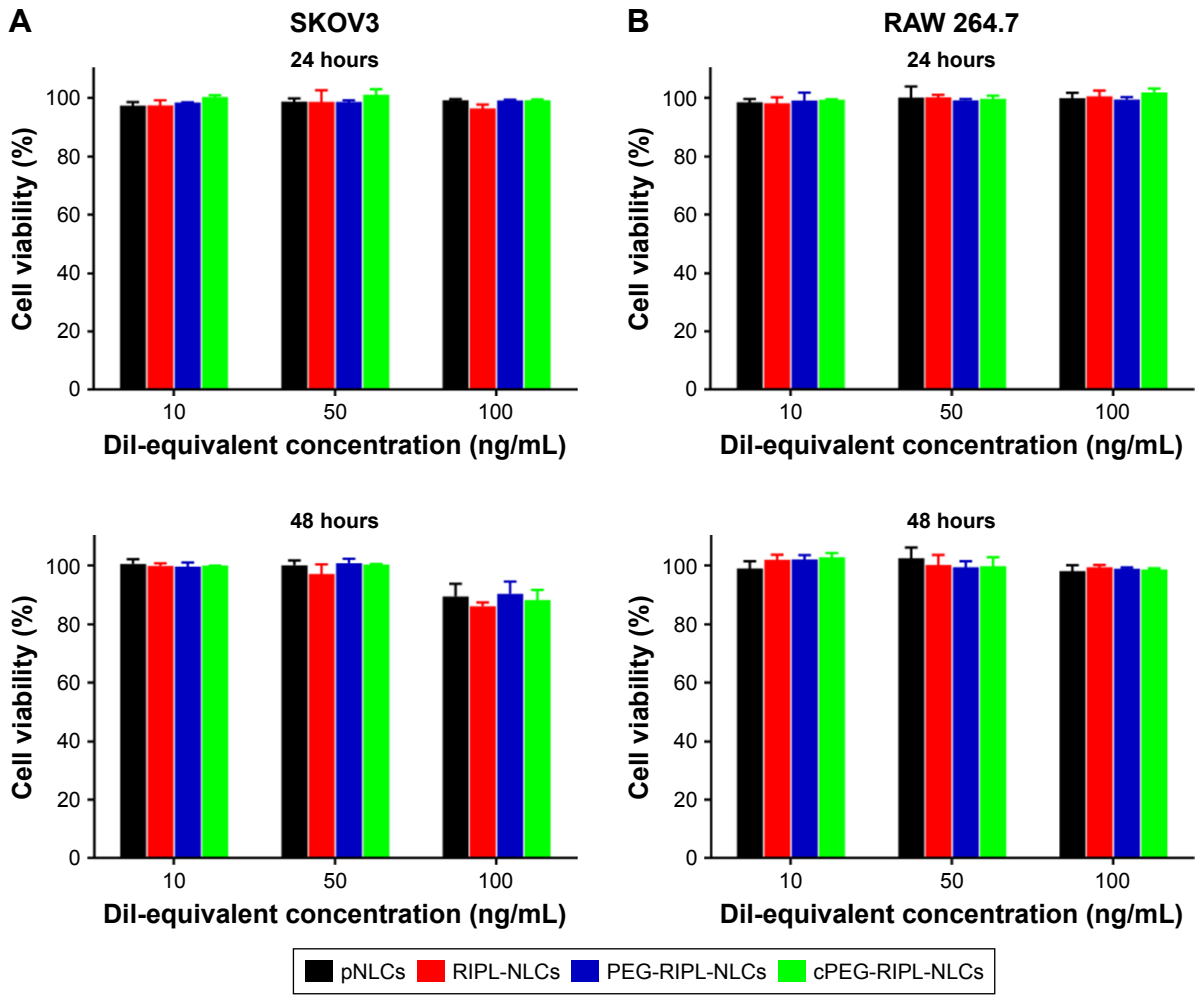

Figure 7 Cytotoxicity of various empty NLC samples in SKOV3 (**A**) and RAW 264.7 (**B**) cell lines at different DiI-equivalent concentrations.
Note: Data represent the means±SD (n=3).
Abbreviations: NLC, nanostructured lipid carrier; pNLCs, plain NLCs; RIPL-NLCs, RIPL peptide-conjugated NLCs; PEG-RIPL-NLCs, PEG-modified RIPL-NLCs; cPEG-RIPL-NLCs, cleavable PEG-modified RIPL-NLCs.

that was employed for cellular uptake and phagocytosis studies, none of the NLCs caused any significant cytotoxicity to either cell line. NLCs are generally recognized as safe,[41] and RIPL-NLCs used in our previous study did not cause any cytotoxicity issues.[4] In addition, PEGylation is well recognized as a biocompatible and safe derivatization.[4,42] Thus, we concluded that all NLC systems used in this study were nontoxic for both cell types.

Tumor spheroid penetration

As a mainstream assay, the in vitro two-dimensional (2D) monolayer culture model has been frequently utilized, with associated internalization studies providing a prediction of the performance of nanocarrier systems in vivo.[43] However, the 2D-model does not accurately reflect the complexity of actual tumor tissues. Alternatively, the 3D-tumor spheroid model has been recently introduced as an intermediate because of the possibility to closely simulate the pathological conditions such as complex extracellular matrix, regions of heterogenous cellular growth, as well as pH, nutrient, and oxygen gradients,[44,45] although this model has limitations of requiring longer culture time for growth and a lack of vascularity.[46] Nevertheless, it is also possible to observe the accumulation and penetration of nanoparticles depth-wise throughout the spheroid structure.[47]

Here, to evaluate the penetrating ability of NLC formulations into avascular solid tumors, we established in vitro SKOV3 3D spheroids and observed the distribution of DiI throughout the spheroids using CLSM (Figure 8). The size of spheroids varied from 250 to 750 µm by simply controlling the seeding quantity of cells.[48] The spheroids between 400 and 600 µm could develop the oxygen and nutrient gradients.[49] In this study, the spheroids were grown to ~500 µm to ensure a homogenous morphology with high reproducibility. Different layers of spheroids could be seen from the Z-stack images, with increasing depth from the left to the right. As expected, the Z-stacked images of spheroids suggested that exposure of the RIPL peptide enhanced the penetration into the tumor spheroid, whereas the presence of PEG on the NLC surface hindered the penetration. Among the NLCs tested, RIPL-NLCs showed the highest DiI accumulation throughout the spheroids. The fluorescence could be observed as deep as 45–60 µm in the core of the SKOV3 tumor spheroid. These results were consistent with earlier reports wherein nanocarrier systems modified with a cell-penetrating peptide such as R8 or TAT showed

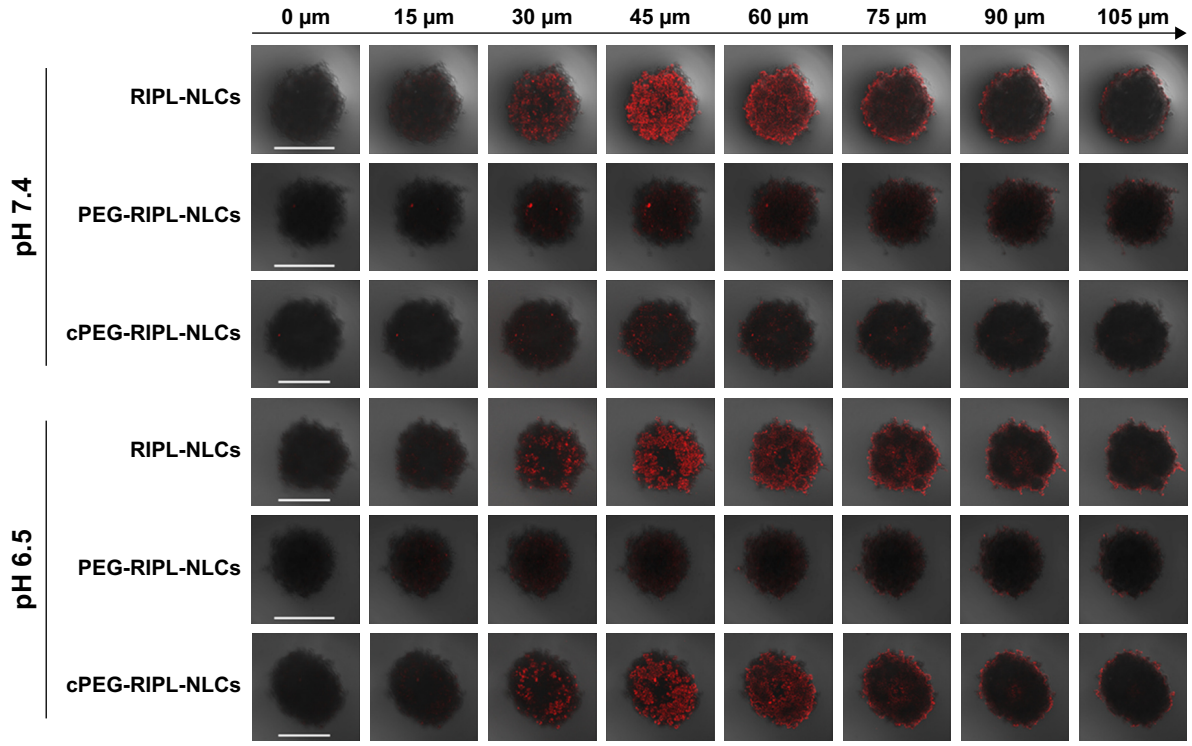

Figure 8 Penetration of DiI-loaded NLC samples through SKOV3 tumor spheroids at pH 6.5 and 7.4 for 2 hours.
Notes: Z-stack images were obtained from the top toward the tumor spheroid equatorial plane in 15 µm intervals. Scale bar represents 500 µm.
Abbreviations: DiI, 1,1′-dioctadecyl-3,3,3′,3′-tetramethylindocarbocyanine perchlorate; NLC, nanostructured lipid carrier; pNLCs, plain NLCs; RIPL-NLCs, RIPL peptide-conjugated NLCs; PEG-RIPL-NLCs, PEG-modified RIPL-NLCs; cPEG-RIPL-NLCs, cleavable PEG-modified RIPL-NLCs.

a strong ability for cell internalization.[50,51] In comparison, PEG-RIPL-NLCs exhibited limited penetration in SKOV3 spheroids, because the PEG modification restricted the RIPL peptide exposure on the surface as described in the cell uptake experiment, with comparable PEG shielding effects observed for both pHs. However, cPEG-RIPL-NLCs showed a pH-dependency with regard to spheroid penetration. At pH 7.4, cPEG-RIPL-NLCs could not penetrate deep into the core region of the spheroid over 2 hours, exhibiting a weak fluorescence throughout the spheroid. Conversely, at pH 6.5, cPEG-RIPL-NLCs showed high fluorescence intensity in the core region, comparable to that of the RIPL-NLC-treated group, indicating the pH-sensitive detachment of cPEG. These advantages of cPEG-RIPL-NLCs indicated good potential for the development of a targetable nanocarrier system that efficiently accumulates into tumor tissues in vivo. However, additional studies regarding nanocarrier in vivo biodistribution following intravenous administration are still needed. Moreover, instead of pH-labile Hz bond, relatively stable bonds including the disulfide bond should be evaluated in the future.

Conclusion

cPEG-RIPL-NLCs were successfully designed by employing DPPE-Hz-PEG$_{3000}$ as a cPEG to RIPL-NLCs and evaluated for steric stabilization and cell uptake characteristics in vitro. With a grafting density of 5 mol% PEG, the plasma protein adsorption was efficiently controlled, and the macrophage uptake was minimized. The cleavage of PEG chains was pH-sensitive and time dependent, resulting in de-shielding of RIPL peptides on the NLC surface. Using DiI as a fluorescent probe, enhanced intracellular uptake in SKOV3 cells and 3D-tumor spheroids was demonstrated. Therefore, we concluded that cPEG-RIPL-NLCs may serve as a good candidate for development as an in vivo Hpn-selective drug delivery agent for cancer therapy.

Acknowledgment

This work was supported by the National Research Foundation of Korea (NRF) grant funded by the Korea government (MSIP) (No 2016R1A2B4011449).

Disclosure

The authors report no conflicts of interest in this work.

References

1. Jaiswal P, Gidwani B, Vyas A. Nanostructured lipid carriers and their current application in targeted drug delivery. *Artif Cells Nanomed Biotechnol*. 2016;44(1):27–40.
2. Wang G, Wang J, Wu W, Tony To SS, Zhao H, Wang J. Advances in lipid-based drug delivery: enhancing efficiency for hydrophobic drugs. *Expert Opin Drug Deliv*. 2015;12(9):1475–1499.
3. Liu D, Zhang N. Cancer chemotherapy with lipid-based nanocarriers. *Crit Rev Ther Drug Carrier Syst*. 2010;27(5):371–417.
4. Lee SG, Kim CH, Sung SW, et al. RIPL peptide-conjugated nanostructured lipid carriers for enhanced intracellular drug delivery to hepsin-expressing cancer cells. *Int J Nanomedicine*. 2018;13:3263–3278.
5. Shi J, Kantoff PW, Wooster R, Farokhzad OC. Cancer nanomedicine: progress, challenges and opportunities. *Nat Rev Cancer*. 2017;17(1):20–37.
6. Owens DE, Peppas NA. Opsonization, biodistribution, and pharmacokinetics of polymeric nanoparticles. *Int J Pharm*. 2006;307(1):93–102.
7. Che J, Okeke CI, Hu ZB, Xu J. DSPE-PEG: a distinctive component in drug delivery system. *Curr Pharm Des*. 2015;21(12):1598–1605.
8. Kim CH, Lee SG, Kang MJ, Lee S, Choi YW. Surface modification of lipid-based nanocarriers for cancer cell-specific drug targeting. *J Pharm Investig*. 2017;47(3):203–227.
9. Fang Y, Xue J, Gao S, et al. Cleavable PEGylation: a strategy for overcoming the "PEG dilemma" in efficient drug delivery. *Drug Deliv*. 2017;24(Suppl 1):22–32.
10. Koren E, Apte A, Jani A, Torchilin VP. Multifunctional PEGylated 2C5-immunoliposomes containing pH-sensitive bonds and TAT peptide for enhanced tumor cell internalization and cytotoxicity. *J Control Release*. 2012;160(2):264–273.
11. Zhang L, Wang Y, Yang Y, et al. High tumor penetration of paclitaxel loaded pH sensitive cleavable liposomes by depletion of tumor collagen I in breast cancer. *ACS Appl Mater Interfaces*. 2015;7(18):9691–9701.
12. Ding Y, Sun D, Wang GL, et al. An efficient PEGylated liposomal nanocarrier containing cell-penetrating peptide and pH-sensitive hydrazone bond for enhancing tumor-targeted drug delivery. *Int J Nanomedicine*. 2015;10:6199–6214.
13. Bruun J, Larsen TB, Jølck RI, et al. Investigation of enzyme-sensitive lipid nanoparticles for delivery of siRNA to blood-brain barrier and glioma cells. *Int J Nanomedicine*. 2015;10:5995–6008.
14. Hatakeyama H, Akita H, Ito E, et al. Systemic delivery of siRNA to tumors using a lipid nanoparticle containing a tumor-specific cleavable PEG-lipid. *Biomaterials*. 2011;32(18):4306–4316.
15. Kulkarni PS, Haldar MK, Nahire RR, et al. Mmp-9 responsive PEG cleavable nanovesicles for efficient delivery of chemotherapeutics to pancreatic cancer. *Mol Pharm*. 2014;11(7):2390–2399.
16. Mcneeley KM, Karathanasis E, Annapragada AV, Bellamkonda RV. Masking and triggered unmasking of targeting ligands on nanocarriers to improve drug delivery to brain tumors. *Biomaterials*. 2009;30(23–24):3986–3995.
17. Oumzil K, Khiati S, Grinstaff MW, Barthélémy P. Reduction-triggered delivery using nucleoside-lipid based carriers possessing a cleavable PEG coating. *J Control Release*. 2011;151(2):123–130.
18. Wang H, Sun M, Li D, Yang X, Han C, Pan W. Redox sensitive PEG controlled octaarginine and targeting peptide co-modified nanostructured lipid carriers for enhanced tumour penetrating and targeting in vitro and in vivo. *Artif Cells Nanomed Biotechnol*. 2018;46(2):313–322.
19. Mo R, Gu Z. Tumor microenvironment and intracellular signal-activated nanomaterials for anticancer drug delivery. *Mater Today*. 2016;19(5):274–283.
20. Gullotti E, Yeo Y. Extracellularly activated nanocarriers: a new paradigm of tumor targeted drug delivery. *Mol Pharm*. 2009;6(4):1041–1051.
21. Romberg B, Hennink WE, Storm G. Sheddable coatings for long-circulating nanoparticles. *Pharm Res*. 2008;25(1):55–71.
22. Kang MH, Park MJ, Yoo HJ, et al. RIPL peptide (IPLVVPLRRRRRRRRC)-conjugated liposomes for enhanced intracellular drug delivery to hepsin-expressing cancer cells. *Eur J Pharm Biopharm*. 2014;87(3):489–499.
23. Wang C, Wang X, Zhong T, et al. The antitumor activity of tumor-homing peptide-modified thermosensitive liposomes containing doxorubicin on MCF-7/ADR: in vitro and in vivo. *Int J Nanomedicine*. 2015;10:2229–2248.

24. Kale AA, Torchilin VP. Design, synthesis, and characterization of pH-sensitive PEG-PE conjugates for stimuli-sensitive pharmaceutical nanocarriers: the effect of substitutes at the hydrazone linkage on the ph stability of PEG-PE conjugates. *Bioconjug Chem*. 2007;18(2):363–370.
25. Luo Q, Zhao J, Zhang X, Pan W. Nanostructured lipid carrier (NLC) coated with Chitosan Oligosaccharides and its potential use in ocular drug delivery system. *Int J Pharm*. 2011;403(1–2):185–191.
26. Shin DH, Xuan S, Kim W-Y, Bae G-U, Kim J-S. CD133 antibody-conjugated immunoliposomes encapsulating gemcitabine for targeting glioblastoma stem cells. *J Mater Chem B*. 2014;2(24):3771–3781.
27. Glorani G, Marin R, Canton P, et al. Pegylated silica nanoparticles: cytotoxicity and macrophage uptake. *J Nanoparticle Res*. 2017;19(8):294.
28. Shen M, Huang Y, Han L, et al. Multifunctional drug delivery system for targeting tumor and its acidic microenvironment. *J Control Release*. 2012;161(3):884–892.
29. Yoon HY, Kwak SS, Jang MH, et al. Docetaxel-loaded RIPL peptide (IPLVVPLRRRRRRRRC)-conjugated liposomes: drug release, cytotoxicity, and antitumor efficacy. *Int J Pharm*. 2017;523(1):229–237.
30. Baek N, Seo OW, Kim M, Hulme J, An SS, Ssa A. Monitoring the effects of doxorubicin on 3D-spheroid tumor cells in real-time. *Onco Targets Ther*. 2016;9:7207–7218.
31. Rabanel JM, Hildgen P, Banquy X. Assessment of PEG on polymeric particles surface, a key step in drug carrier translation. *J Control Release*. 2014;185:71–87.
32. Tang J, Fu H, Kuang Q, et al. Liposomes co-modified with cholesterol anchored cleavable PEG and octaarginines for tumor targeted drug delivery. *J Drug Target*. 2014;22(4):313–326.
33. Sawant RM, Hurley JP, Salmaso S, et al. "SMART" drug delivery systems: double-targeted pH-responsive pharmaceutical nanocarriers. *Bioconjug Chem*. 2006;17(4):943–949.
34. Essa S, Rabanel JM, Hildgen P. Characterization of rhodamine loaded PEG-g-PLA nanoparticles (NPs): effect of poly(ethylene glycol) grafting density. *Int J Pharm*. 2011;411(1–2):178–187.
35. Jang MH, Kim CH, Yoon HY. Steric stabilization of RIPL peptide-conjugated liposomes and in vitro assessment. *J Pharm Investig*. 2018;54(1):1–11.
36. Howard MD, Jay M, Dziubla TD, Lu X. PEGylation of nanocarrier drug delivery systems: state of the art. *J Biomed Nanotechnol*. 2008;4(2):133–148.
37. Li SD, Huang L. Stealth nanoparticles: high density but sheddable PEG is a key for tumor targeting. *J Control Release*. 2010;145(3):178–181.
38. Liu Y, Ran R, Chen J, et al. Paclitaxel loaded liposomes decorated with a multifunctional tandem peptide for glioma targeting. *Biomaterials*. 2014;35(17):4835–4847.
39. Göppert TM, Müller RH. Polysorbate-stabilized solid lipid nanoparticles as colloidal carriers for intravenous targeting of drugs to the brain: comparison of plasma protein adsorption patterns. *J Drug Target*. 2005;13(3):179–187.
40. Wan F, You J, Sun Y, et al. Studies on PEG-modified SLNs loading vinorelbinebitartrate (I): preparation and evaluation in vitro. *Int J Pharm*. 2008;359(1–2):104–110.
41. Lim SB, Banerjee A, Önyüksel H. Improvement of drug safety by the use of lipid-based nanocarriers. *J Control Release*. 2012;163(1):34–45.
42. Immordino ML, Dosio F, Cattel L. Stealth liposomes: review of the basic science, rationale, and clinical applications, existing and potential. *Int J Nanomedicine*. 2006;1(3):297–315.
43. Page H, Flood P, Reynaud EG. Three-dimensional tissue cultures: current trends and beyond. *Cell Tissue Res*. 2013;352(1):123–131.
44. Millard M, Yakavets I, Zorin V, Kulmukhamedova A, Marchal S, Bezdetnaya L. Drug delivery to solid tumors: the predictive value of the multicellular tumor spheroid model for nanomedicine screening. *Int J Nanomedicine*. 2017;12:7993–8007.
45. Huang BW, Gao JQ. Application of 3D cultured multicellular spheroid tumor models in tumor-targeted drug delivery system research. *J Control Release*. 2018;270:246–259.
46. Wan X, Li Z, Ye H, Cui Z. Three-dimensional perfused tumour spheroid model for anti-cancer drug screening. *BiotechnolLett*. 2016;38(8):1389–1395.
47. Wang X, Zhen X, Wang J, Zhang J, Wu W, Jiang X. Doxorubicin delivery to 3D multicellular spheroids and tumors based on boronic acid-rich chitosan nanoparticles. *Biomaterials*. 2013;34(19):4667–4679.
48. Perche F, Torchilin VP. Cancer cell spheroids as a model to evaluate chemotherapy protocols. *Cancer BiolTher*. 2012;13(12):1205–1213.
49. Breslin S, O'Driscoll L. Three-dimensional cell culture: the missing link in drug discovery. *Drug Discov Today*. 2013;18(5–6):240–249.
50. Biswas S, Deshpande PP, Perche F, Dodwadkar NS, Sane SD, Torchilin VP. Octa-arginine-modified pegylated liposomal doxorubicin: an effective treatment strategy for non-small cell lung cancer. *Cancer Lett*. 2013;335(1):191–200.
51. Mei L, Fu L, Shi K, et al. Increased tumor targeted delivery using a multistage liposome system functionalized with RGD, TAT and cleavable PEG. *Int J Pharm*. 2014;468(1–2):26–38.